Available online at www.sciencedirect.com

ScienceDirect

Procedia Structural Integrity 2 (2016) 316–325

Structural Integrity Procedia

www.elsevier.com/locate/procedia

21st European Conference on Fracture, ECF21, 20-24 June 2016, Catania, Italy

Cohesive and XFEM evaluation of adhesive failure for dissimilar single-lap joints

Florin Adrian Stuparu[a], Dragos Alexandru Apostol[a], Dan Mihai Constantinescu[a]*
Catalin Radu Picu[b], Marin Sandu[a], Stefan Sorohan[a]

[a]*University POLITEHNICA of Bucharest, 060042 Bucharest, Romania*
[b]*Rensselaer Polytechnic Institute, 12180 Troy, NY USA*

Abstract

Cohesive Zone Modelling (CZM) and eXtended Finite Element Modelling (XFEM) available in Abaqus® are used together to simulate the behaviour and strength of dissimilar single-lap adhesively bonded joints. A distinct CZM model is also used. Single-lap joints made of aluminium and carbon fibre adherends of different thickness are tested to understand better the behaviour of such dissimilar joints. Local deformation fields are monitored by using the digital image correlation method (DIC). Peeling and shearing strains are investigated, emphasizing that peeling is important in the region where failure is initiated, towards an extremity of the overlap region. The use of dissimilar adherends is reducing the strength and stiffness of the joints as the delamination and pull-out of the carbon fibres reduces the integrity of the joint. The experimental evidence given by DIC is not to be obtained by numerical simulations.

Peer-review under responsibility of the Scientific Committee of ECF21.

Keywords: Single-lap joint; Cohesive zone model; Extended finite element method; Aluminium and carbon adherends; Digital image correlation.

1. Introduction

In engineering structural integrity applications the presence of imperfections can reduce significantly the load bearing capacity. Without a better understanding of progressive failure, the fracture criteria and predictive capabilities will be limited. Interface cracking is generally a mixed mode cracking, as both normal and shear stresses

* Corresponding author. Tel.: +40-21-402-9210; fax: +40-21-402-9213.
E-mail address: dan.constantinescu@upb.ro

Peer review under responsibility of the Scientific Committee of ECF21.
10.1016/j.prostr.2016.06.041

develop. Experiments have shown that fracture energy can depend on mode mixity, as shown by Cao and Evans (1989), Wang and Suo (1990), Liechti and Chai (1992). A comprehensive literature review on the types of tests used for adhesive joints for single and mixed-mode fracture, underlining their advantages and disadvantages, was done by Chavez et al. (2014). They concluded that there is no general agreement about the test suitability for mixed-mode fracture assessment of adhesive joints.

In the present paper two numerical methods and an experimental one will be used. The developments of these approaches are presented briefly.

1.1. Cohesive zone modelling

During the crack growth process, two new surfaces are created. Before the physical crack is formed, these two surfaces are held together by traction within a cohesive zone. A cohesive law is also denoted a traction-separation law. The cohesive zone modelling (CZM) approach has emerged as a powerful analytical tool for nonlinear fracture processes.

Cohesive zone models have particularly been used to analyze composite delamination problems. Cohesive strength and fracture energy are believed to have greater importance with respect to the specific shape chosen for the cohesive model. Most damage models, such as the Progressive Damage Model for Composites provided in Abaqus® (2008) and typical cohesive elements as presented by Camanho et al. (2003), Turon et al. (2006), and Dávila et al. (2009), represent the evolution of damage with linear softening laws that are described by a maximum traction and a critical energy release rate. As discussed the shape of the softening law, e.g., linear or exponential, is generally assumed to be inconsequential for the prediction of fracture for small-scale bridging conditions, but plays a fundamental role in the prediction of fracture under large-scale bridging conditions, where the process zone length may be large relative to other length scales in the problem.

FEM analyses of single-lap joints were performed by Kafkalidis and Thouless (2002) using a CZM approach and allowing the cohesive properties of the interface and plastic deformation of the adherends to be included in the analysis by means of a traction–separation law with a trapezoidal shape. Using cohesive-zone parameters determined for the particular combination of materials, the numerical predictions for different bonded shapes were confirmed by the experimental observations. The numerical models predicted accurately the failure loads, displacements and deformations of the joints.

1.2. Extended finite element modelling

The recently developed eXtended Finite Element Method (XFEM) is an extension of the FEM, and its fundamental features were described by Belytschko and Black (1999), based on the idea of partition of unity presented by Melenk and Babuska (1996), which consists on local enrichment functions for the nodal displacements to model crack growth and separation between crack faces. With this technique, discontinuities such as cracks are simulated as enriched features, by allowing discontinuities to grow through the enrichment of the degrees of freedom of the nearby nodes with special displacement functions. As the crack tip changes its position and path due to loading conditions, the XFEM algorithm creates the necessary enrichment functions for the nodal points of the finite elements around the crack path/tip. Compared to CZMs, XFEM excels in simulating crack onset and growth along an arbitrary path without the requirement of the mesh to match the geometry of the discontinuities neither remeshing near the crack as done by Campilho et al. (2011). This can be an advantage to CZM modelling for the simulation of bonded engineering plastics or polymer–matrix composites, where adherend cracking may occur after initiation in the adhesive. CZM has a strong intrinsic limitation since cohesive elements to simulate damage growth must be placed at the growth lines where damage is supposed to occur. If damage would occur in another region(s), the correct results would not be provided. However, this limitation is usually of little importance as damage growth in adhesively bonded joints or structures is many times limited to typical locations such as the adhesive/adherend interfaces or within the adhesive itself. This does not occur with the XFEM, as crack propagation is allowed anywhere within the models. However, when speaking about the XFEM formulation of Abaqus®, another drawback appears, because the prediction of damage initiation is based on one value of strength/strain which gives damage initiation (by the maximum principal stress or strain criterion, respectively).

1.3. Digital image correlation method

The digital image correlation (DIC) method has inspired several researchers for CZM identification and to analyze the strength of lap-joints. When dealing with classical CZM based on DIC techniques, researches are limited to an identification of the cohesive parameters when the cohesive law is a priori fully or partly given, and/or for predefined crack paths (debond of interfaces) or precracked samples. Only as examples, Valoroso and Fedele (2010) identified the mode I parameters of a cohesive zone model for the analysis of adhesive joints and Shen and Paulino (2011) provided a full-field DIC algorithm to compute the smooth and continuous displacement field, which is then used as input to a finite element model for inverse analysis through an optimization procedure in order to compute the cohesive properties of a ductile adhesive. Richefeu et al. (2012) proposed a CZM evaluation based on DIC full-field measurements. They showed that their identification does not assume neither any particular shape nor any predefined crack path, but focuses on the experimental validity of the projection of volumic (micro) damage onto a simple surface. However, the study is restricted to metallic materials subjected to uniaxial tension.

Moreira and Nunes (2014) investigated the behaviour of a flexible adhesive and the critical shearing deformations which decrease towards the ends of the overlap, suggesting that the peeling strains are responsible for the initiation of the failure. They pointed out that it is essential to consider the peeling effects for the correct interpretation of the strength of the joint. Moutrille et al. (2009), Nunes and Moreira (2013, and Silva and Nunes (2014) used also DIC for studying several geometrical configurations and successfully analyzed the influence of the aforementioned different parameters on the shearing strength of the joints.

2. Single-lap configurations and materials

The single-lap joints used in the investigations have the geometry presented in Fig. 1. The thickness of the adhesive is kept constant to 0.5 mm and the effective overlap length is L = 20 mm.

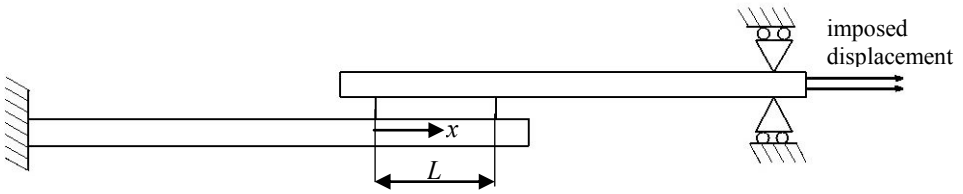

Fig. 1. The single-lap joint geometry.

At the ends of the overlap a 5 mm gap length is kept on each side of the overlap as used to control the thickness of the adhesive layer with a wax layer of 0.5 mm, as it was done in the experimental preparation of the specimens.

The adhesive used in the simulations is Araldite® 2015 (Huntsman Advanced Materials, Basel, Switzerland) with some of its mechanical properties considered as suggested by Campilho et al. (2012) and specified in Table 1. This adhesive has a ductile behaviour. The adherends had the conventional corresponding mechanical properties are given in the same table. The considered thicknesses of the adherends were either 3 mm or 5 mm, having a width of 30 mm, and a length of 150 mm.

Table 1. Some mechanical properties of the adhesive and the aluminium adherend used in simulations.

		Araldite® 2015	Aluminium
Young's modulus [MPa]	E	1850*	70000
Shear modulus [MPa]	G	560	26340
Normal traction at initiation [MPa]	σ_n^0	21.6	230
Shearing traction at initiation [MPa]	σ_s^0	17.9	230
Fracture energy in tension [N/mm]	G_n^c	0.43	15
Fracture energy in shear [N/mm]	G_s^c	4.70	15

* value was modified to 1790 MPa after experimental testing

The elastic constants of Araldite 2015 were established with DIC on bulk specimens as: longitudinal modulus of elasticity E = 1790 MPa and Poisson's ratio ν = 0.32. This adhesive has a ductile behaviour.

The adherends were made from aluminium 6060 T6 and unidirectional carbon fibre of 250 g/m^2 with epoxy resin matrix. The considered thicknesses of the adherends for both materials were either 3 mm or 5 mm, having all of them a width of 30 mm. The adherends were further denoted as *aluminium* and *carbon* having the thickness indicated afterwards. The elastic constants of these adherends were established through traction tests on bulk ISO standardized specimens, as indicated in Table 2. Tests were done on a Zwick Z010 (10 kN) machine. Speed of testing was of 1 mm/min.

Table 2. Elastic constants of adherends.

	Aluminium	Carbon 3 mm	Carbon 5 mm
Modulus of elasticity [MPa]	70000	76000	64000
Poisson's ratio	0.33	0.35	0.37

The increase of stiffness of the 3 mm carbon adherend can be explained due to the higher volume fraction of carbon fibres which resulted for this thickness.

2. CZM and XFEM

2.1. CZM model

As boundary conditions, one adherend was fixed at one end and on the other adherend a displacement was imposed horizontally at the opposite end.

The triangular CZM formulation was chosen for this analysis because of its simplicity, large use for investigation purposes, and availability in FEM package Abaqus® (Providence, RI, USA) including a mixed mode formulation, which is absolutely necessary to model the single-lap joints used hereby. Damage initiation can be specified by different criteria. In this work, the quadratic nominal stress criterion (which states that the sum of the squares of the ratios between the normal and shearing stresses to their values at initiation is equal to 1) was selected for the initiation of damage, as previously used and tested for accuracy by Stuparu et al. (2016).

The two-dimensional meshing of the adhesive was done by using COH2D4 and CPE4 for adherends four-node linear plane strain elements. The adhesive layer was modelled with cohesive elements of 0.5 x 0.5 mm; same size of the elements was used for the adherends. In Fig. 2 the model for a 3 mm thickness adherend is shown.

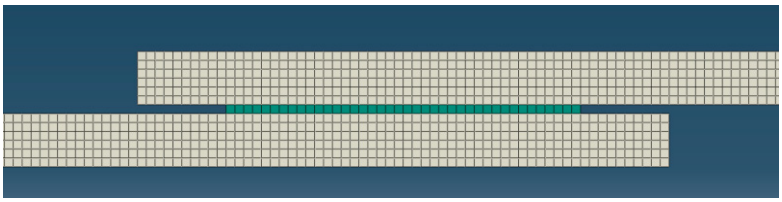

Fig. 2. Cohesive FE model of the single-lap joint.

The variation of stresses can be represented over the length of the adhesive overlap as a function of a normalized coordinate x/L, having values from 0 to 1. Two moments were considered to be important: the initiation of damage in the first cohesive element and the moment of propagation of damage, considered as crack propagation.

2.2. *XFEM-cohesive model*

Adhesive and adherends have been modelled by using the XFEM capabilities. Using this technique, damage takes place when the principal stress/strain is greater than the limit value specified in the traction–separation low. In

this study a strain criterion was chosen for damage initiation and the crack propagates orthogonally to the maximum principal strain using a fracture energy criterion. The critical strain was established experimentally through traction tests, Stuparu et al. (2016). Fracture at bonded interfaces was modelled by defining a tie constraint between the adherent and the adhesive material (local approach). The tie constraint approach allows to model zero-thickness cohesive layer using a finer discretization than that of the bulk material and may be more desirable in certain modelling situations. The same material properties used for XFEM were also used for cohesive interface modelling. Only the initial stiffness value used for the cohesive elements at the interface was changed. The initially considered value was 10^6 N/mm^3, as suggested in the literature, Camanho et al. (2003), but later was diminished to 10^4 N/mm^3 as to improve the convergence issues. The zero-thickness cohesive layer damage takes place according to the quadratic nominal stress criterion and the crack propagates using power low mixed mode fracture energy behaviour.

The geometry of the single-lap joint to be analyzed with the combined XFEM-cohesive model is presented in Fig. 3. The active overlap length is L = 20 mm as before and at both ends symmetric 5 mm length delaminations were introduced in the middle of the adhesive layer of 1 mm thickness. Their role is to facilitate the initiation and propagation of damage. Imposed boundary conditions are the same as before (Fig. 1).

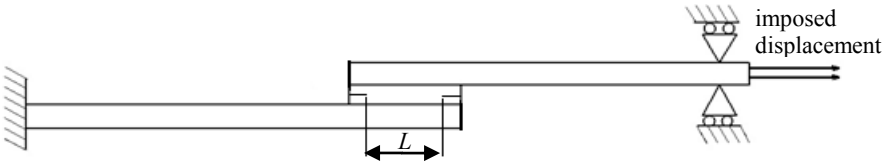

Fig. 3. Single-lap joint geometry with lateral delaminations.

The adherends and adhesive were modelled with XFEM by using the plane strain element CPE4 of size 0.2x0.2 mm. For optimizing the calculations the adherends were modelled with the same elements by using the *bias* function from Abaqus® which enables the increase of the size of the elements from 0.2x0.2 mm to 0.2x1 mm as to be noticed in Fig. 4. Hereby the behaviour of the adhesive and the adherends is linear elastic.

Zero-thickness cohesive elements are considered at the interface between the adhesive and the adherend.

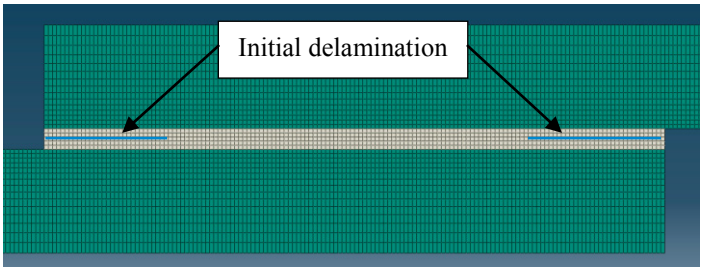

Fig. 4. XFEM-cohesive FE model

The force-displacement curve obtained numerically is shown in Fig. 5. The important moments are: 1. initiation of damage (crack); 2. propagation by XFEM through the adhesive to the interface; 3. failure in the cohesive elements at the interface through delamination.

After propagation the crack remains at the interface and doesn't move back to the adhesive, nor into the adherent. The XFEM is not effective any more. Cohesive elements of zero thickness take over the increase of the delamination up to the failure of the joint (point 3 in Fig. 5).

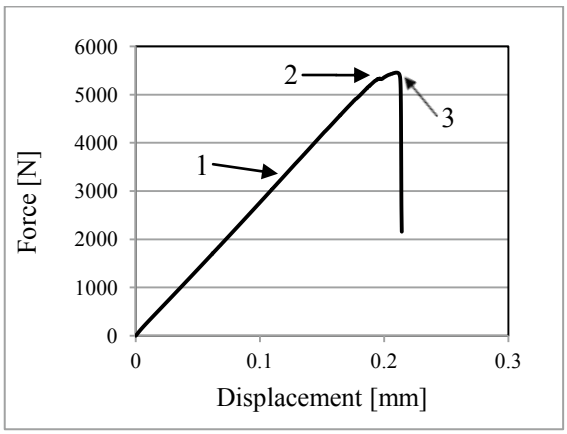

Fig. 5. Force-displacement curve for the given geometry.

As an example, at initiation, the peeling stress and the shearing stress variations are shown in Fig. 6a), respectively Fig. 6b).

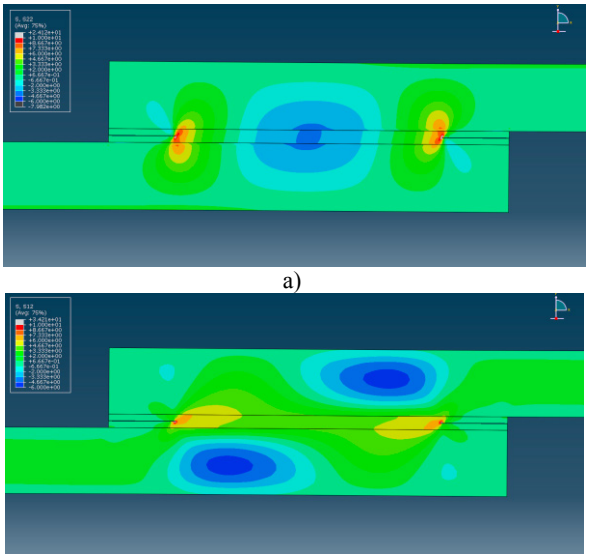

Fig. 6. Variation of stresses at damage initiation: a) peeling stress; b) shearing stress

3. Digital image correlation method

The single-lap joint prepared for DIC measurements is shown in Fig. 7. On the left side it is better noticed the uneven surface due to the wax of constant 0.5 mm thickness which filled the overlap for 5 mm on each side as to control the adhesive thickness. In all, six different geometrical configurations were used for testing, aluminium-aluminium, aluminium-carbon, and carbon-carbon, with thicknesses of 3 and 5 mm. If the failure was not cohesive the test was disregarded.

The relative displacements between the adherends were monitored in the overlap region and both peeling and shearing deformations were measured by using DIC. For each configuration out of the five performed tests only the representative one was chosen for further comparisons. Plots of the shearing stress as a function of the displacement between the grips as indicated by the testing machine were also represented.

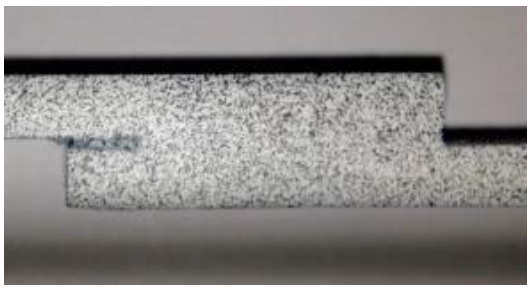

Fig. 7. Surface of a single-lap joint prepared for DIC measurements.

The lateral surface of the single-lap joint was analyzed by using DIC. The ARAMIS 2M system was used to measure the deformations of the adhesive. For all tests a calibre of 35 x 28 mm was considered. One frame per second was acquired. In order to obtain a map of the deformations along the overlap length three virtual gauges were chosen on each side of the overlap as seen in Fig. 8. Top and bottom gauges are positioned on the edges of the adhesive layer. The relative displacements of the adherends are measured along the x axis as to investigate the peeling deformation and the corresponding strain, and along the y axis to monitor the shearing displacement of the adherends and the shearing strain.

Local peeling strains are shown with their values in Fig. 8, both adherends being aluminium of 5 mm thickness. A maximum strain of about 9 % was obtained at the lower extremity of the adhesive shortly before the failure of the joint. The edge parts of 5 mm which contain the wax have been removed from the plot. As getting towards the middle region of the overlap compression is produced in the adhesive, thus indicating the bending of the adherends.

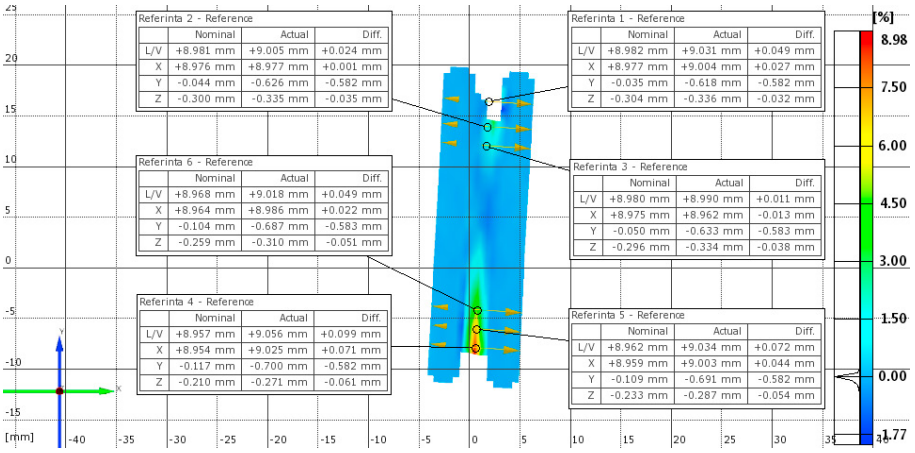

Fig. 8. Peeling strains in the adhesive for an aluminium-aluminium joint.

A similar plot, but this time for the shearing strains of an aluminium-carbon joint, is represented in Fig. 9. It is to be underlined that at the interface the strains have a waiving trajectory thus indicating that the local phenomena of bending and debonding.

It was observed during testing that the strength of the joint is in fact dictated by the interface strength of the carbon laminas and not by the cohesive strength of the adhesive. If the interface strength is assumed to be constant regardless the thickness of the carbon adherends it results that a lower stiffness will lead to a higher peeling force as the thickness of the adherend is decreased. During experiments the pull-out of the carbon fibres due to the interlaminar failure of the adherend was evident.

It is also recommended to avoid any mechanical machining or scratching on the surface of the carbon adherend as to increase its roughness prior to the application of the adhesive. This may also contribute to the unexpected interlaminar failure.

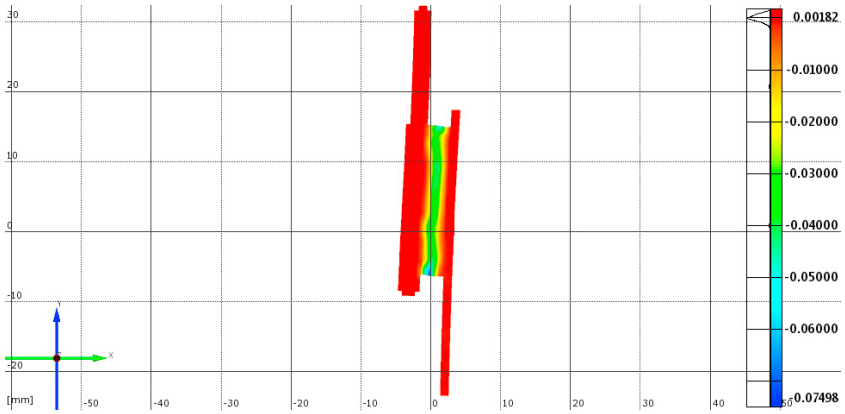

Fig. 9. Shearing strains in the adhesive for an aluminium-carbon joint.

4. Comparison of numerical and experimental results

For adherends of 5 mm thickness the shearing failure stress is about 16 MPa regardless the joint configuration (Fig. 10). Following the forces and displacements indicated by the testing machine the corresponding curves are shown in Fig. 10 for the three combinations of adherends. A slightly larger displacement until failure is obtained for the aluminium-aluminium lap joint, as it has a more ductile behaviour. The aluminium-carbon lap joint is stiffer and probably due to the combination of dissimilar materials fails sooner.

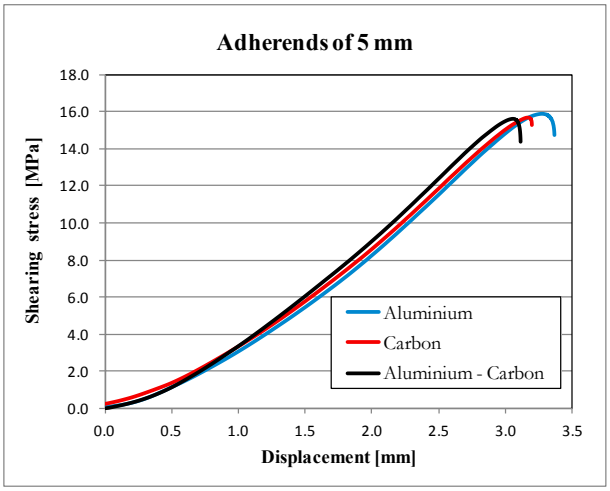

Fig. 10. Influence of material combinations for 5 mm adherend thickness.

The global values of the displacements of the single-lap joint measured by the displacement of the grips of the testing machine is at failure about 3 mm for the 5 mm adherends, and about the same value or less for the 3 mm adherends (not less than 2.5 mm). This globally maximum measured displacement is significantly larger than the local relative displacements of the aluminium adherends measured on x and y directions (Fig. 8) with DIC, as 0.07 mm on x (bottom virtual gauge), respectively about the same in any virtual gauge as 0.6 mm on y direction. Only the local relative displacements are reflecting the correct behaviour of the adhesive.

In Fig. 11 are presented the results of numerical simulations obtained with the CZM model and XFEM-CZM model and the experimental results of four tests for aluminium-carbon adherends of 5 mm. Local vertical displacements are measured with DIC over a virtual gage length of 50 mm which was emulated symmetrically with respect to the overlap length.

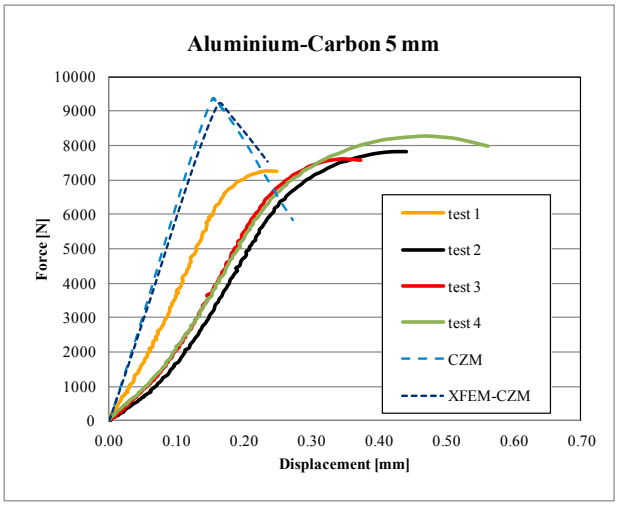

Fig. 11. Local force-displacement diagrams obtained numerically and experimentally for an aluminium-carbon joint.

The behaviour of the joint obtained through numerical simulations indicates a stiffer assembly which fails sooner at about 9000 N. The experimental tests give a more ductile behaviour of the dissimilar joint able to withstand a maximum force of about 8000 N (with one exception) with displacements at failure in between 0.35-0.55 mm. However these displacements at failure are far away from the ones which are greater than 3 mm as given by the indications of the testing machine (Fig. 10).

For the carbon-carbon single-lap joint with 5 mm thickness adherends the local force-displacement curves obtained experimentally show even a greater scatter than before, as to be seen in Fig. 12. Obviously the interface failure in carbon laminas and pull-out of the fibres (as noticed experimentally) do influence the global behaviour of the joint. The maximum force keeps around 8000 N, but the displacements at failure are bellow 0.4 mm for all tests.

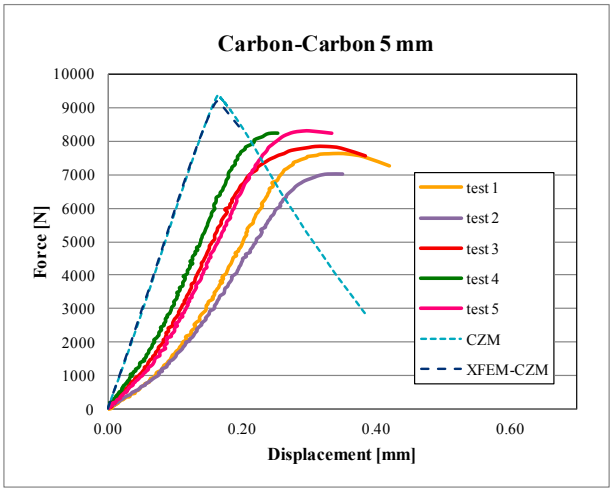

Fig. 12. Local force-displacement diagrams obtained numerically and experimentally for an carbon-carbon joint.

5. Conclusions

Combined CZM and XFEM-CZM numerical and DIC experimental analyses on the behaviour of dissimilar single-lap joints are reported in this article. For the same type and thickness of the adhesive and same overlap length

we analyze the influence of the material of the adherends and their thickness. The dissimilar aluminium-carbon and carbon-carbon joints are of special interest as the numerical analyses of their strength overestimate the experimental evidence given by DIC.

Digital image correlation measurements done in the immediate vicinity of the adhesive layer can provide correct information about the shearing and peeling deformations. Dissimilar aluminium-carbon joints succeed to maintain the stiffness of the assembly as compared to the aluminium joints, but their strength is diminished by the pull-out and delamination of carbon fibres. For carbon-carbon single-lap joints both strength and stiffness are diminished as significant additional interlaminar damage compromises the integrity of the joint and leads to premature failure of the assembly.

It is of great importance to rely on local deformation measurements and not on the global ones as indicated by the testing machine, which include also the deformation of the adherends. Only by using such an approach a proper evaluation of adhesive failure is possible.

Acknowledgements

The authors acknowledge the support given by a grant of the Romanian National Authority for Scientific Research, CNDI–UEFISCDI, project number PN-II-PT-PCCA-2011-3.2-0068, contract nr. 206/2012.

References

Abaqus® 6.8., 2008. User's Manual. Dassault Systèmes, Providence, RI, USA.

Belytschko, T., Black, T., 1999. Elastic crack growth in finite elements with minimal remeshing. International Journal of Fracture 45, 601–620.

Camanho, P.P., Dávila, C.G., de Moura, M.F.S.F., 2003. Numerical simulation of mixed-mode progressive delamination in composite materials. Journal of Composite Materials 37, 1415–1438.

Campilho, R.D.S.G., Banea, M.D., Chaves, F.J.P., da Silva, L.F.M., 2011. Extended finite element method for fracture characterization of adhesive joints in pure mode I. Computional Materials Science 50, 1543–1549.

Campilho, R.D.S.G., Banea, M.D., Neto, J.A.B.P., da Silva, L.F.M., 2012. Modelling of single-lap joints using cohesive zone models: effect of the cohesive parameters on the output of the simulations. Journal of Adhesion 88, 513-533.

Cao, H.C, Evans, A.G., 1989. An experimental study of the fracture resistance of bimaterial interfaces, Mechanics of Materials 7, 295–304.

Chaves, F.J.P, de Moura. M.F.S.F., da Silva, L.F.M., Dillard, D.A., Esteves, V., 2014. Fracture mechanics tests in adhesively bonded joints: a literature review, Journal of Adhesion 90, pp. 955–992.

Dávila, C.G., Rose, C.A., Camanho, P.P., 2009. A procedure for superposing linear cohesive laws to represent multiple damage mechanisms in the fracture of composites. International Journal of Fracture 158, 211–223.

Kafkalidis, M.S., Thouless, M.D., 2002. The effects of geometry and material properties on the fracture of single lap-shear joints. International Journal of Solids and Structures 39, 4367–4383.

Liechti, K.M., Chai, Y.S., 1992. Asymmetric shielding in interfacial fracture under in-plane shear. Transactions ASME Journal of Applied Mechanics 59, 295–304.

Melenk, J.M., Babuska, I., 1996. The partition of unity finite element method: basic theory and applications. Seminar fur angewandte Mathematik, Eidgenos- sische Technische Hochschule, Research Report No. 96-01, January, CH-8092 Zurich, Switzerland.

Moreira, D.C., Nunes L.C.S., 2014. Experimental analysis of bonded single lap joint with flexible adhesive. Applied Adhesion Science 2:1.

Moutrille, M.P., Derrien, K., Baptiste, D., Balandraud, X., Grédiac, M., 2009. Through-thickness strain field measurement in a composite/aluminium adhesive joint. Composites Part A: Applied Science and Manufacturing 40, 985–996.

Nunes, L.C.S., Moreira, D.C., 2013. Simple shear under large deformation: Experimental and theoretical analyses. European Journal of Mechanics - A/Solids 42, 315–322.

Richefeu, V., Chrysochoos, A., Huon, V., Monerie, Y., Peyroux, R., Wattrisse, B., 2012. Toward local identification of cohesive zone models using digital image correlation. European Journal of Mechanics - A/Solids 34, 38-51.

Shen, B., Paulino, G.H., 2011. Direct extraction of cohesive fracture properties from digital image correlation: A hybrid inverse technique. Experimental Mechanics 51, 143-146.

Silva, T.C., Nunes, L.C.S., 2014. A new experimental approach for the estimation of bending moments in adhesively bonded single lap joints, International Journal of Adhesion and Adhesives 54, 13–20.

Stuparu, F.A., Apostol, D.A., Constantinescu, D.M., Sandu, M., Sorohan, S., 2016. Failure analysis of dissimilar single-lap joints. Frattura ed Integrità Strutturale 36, 70-78.

Turon, A., Camanho, P.P., Costa, J., Dávila, C.G., 2006. A damage model for the simulation of delamination in advanced composites under variable-mode loading. Mechanics of Materials 38, 1072–1089.

Valoroso, N., Fedele, R., 2010. Characterization of a cohesive-zone model describing damage and de-cohesion at bonded interfaces, sensitivity analysis and mode-I parameter identification. International Journal of Solids and Structures 47, 1666-1677.

Wang, J.S., Suo, Z., 1990. Experimental determination of interfacial toughness using Brazil-nut-sandwich. Acta Metallurgica 38, 1279–1290.